Translational Oncology
www.transonc.com

Volume 3 Number 5 October 2010 pp. 293–306 293

Dynamic Contrast-Enhanced Magnetic Resonance Imaging of Sunitinib-Induced Vascular Changes to Schedule Chemotherapy in Renal Cell Carcinoma Xenograft Tumors[1]

Gilda Gali Hillman*, Vinita Singh-Gupta*, Areen K. Al-Bashir[†,‡], Hao Zhang*, Christopher K. Yunker*, Amit D. Patel*, Seema Sethi[§], Judith Abrams[¶] and E. Mark Haacke[†,‡]

*Department of Radiation Oncology, Barbara Ann Karmanos Cancer Institute, Wayne State University School of Medicine, Detroit, MI, USA; [†]Department of Radiology, Barbara Ann Karmanos Cancer Institute, Wayne State University School of Medicine, Detroit, MI, USA; [‡]Department of Biomedical Engineering, Barbara Ann Karmanos Cancer Institute, Wayne State University School of Medicine, Detroit, MI, USA; [§]Department of Pathology, Barbara Ann Karmanos Cancer Institute, Wayne State University School of Medicine, Detroit, MI, USA; [¶]Integrated Biostatistics Unit, Barbara Ann Karmanos Cancer Institute, Wayne State University School of Medicine, Detroit, MI, USA

Abstract

In an attempt to develop better therapeutic approaches for metastatic renal cell carcinoma (RCC), the combination of the antiangiogenic drug sunitinib with gemcitabine was studied. Using dynamic contrast-enhanced magnetic resonance imaging (DCE-MRI), we have previously determined that a sunitinib dosage of 20 mg/kg per day increased kidney tumor perfusion and decreased vascular permeability in a preclinical murine RCC model. This sunitinib dosage causing regularization of tumor vessels was selected to improve delivery of gemcitabine to the tumor. DCE-MRI was used to monitor regularization of vasculature with sunitinib in kidney tumors to schedule gemcitabine. We established an effective and nontoxic schedule of sunitinib combined with gemcitabine consisting of pretreatment with sunitinib for 3 days followed by four treatments of gemcitabine at 20 mg/kg given 3 days apart while continuing daily sunitinib treatment. This treatment caused significant tumor growth inhibition resulting in small residual tumor nodules exhibiting giant tumor cells with degenerative changes, which were observed both in kidney tumors and in spontaneous lung metastases, suggesting a systemic antitumor response. The combined therapy caused a significant increase in mouse survival. DCE-MRI monitoring of vascular changes induced by sunitinib, gemcitabine, and both combined showed increased tumor perfusion and decreased vascular permeability in kidney tumors. These findings, confirmed histologically by thinning of tumor blood vessels, suggest that both sunitinib and gemcitabine exert antiangiogenic effects in addition to cytotoxic antitumor activity. These studies show that DCE-MRI can be used to select the dose and schedule of antiangiogenic drugs to schedule chemotherapy and improve its efficacy.

Translational Oncology (2010) 3, 293–306

Introduction

Recent developments in antiangiogenic therapy have improved targeting metastatic renal cell carcinoma (RCC). The incidence of RCC has increased in recent years, with approximately 54,390 new cases each year in the United States. The disease is responsible for an estimated 13,010 deaths each year [1]. Nearly half of the patients present with localized disease that can be treated by surgical removal [2,3].

Address all correspondence to: Gilda Gali Hillman, PhD, Department of Radiation Oncology, 515 Hudson-Webber Cancer Research Center, 4100 John R. Rd, Detroit, MI 48201. E-mail: hillmang@karmanos.org

[1]This study was supported by Pfizer grant IIR no. GA61818Z 9 (to G.G. Hillman), Karmanos Cancer Institute Pilot Project Grant, and the Fund for Cancer Research.
Received 28 April 2010; Revised 26 June 2010; Accepted 26 June 2010

DOI 10.1593/tlo.10136

However, one third of the patients have metastatic disease at first presentation, and 20% to 30% of the patients treated for localized RCC subsequently develop metastatic disease that frequently involves the lungs [2,3].

The drug sunitinib (SU11248 or Sutent) is a small molecule receptor tyrosine kinase (RTK) inhibitor that has been approved by the US Food and Drug Administration in January 2006 for RCC treatment based on significant responses in multiple metastatic sites and in primary tumors in initial clinical trials for metastatic RCC [4]. We and others have demonstrated that sunitinib targets and inhibits signaling of several RTKs including platelet-derived growth factor receptor, vascular endothelial growth factor receptor, c-kit protooncogene, and FMS-like tyrosine kinase 3 in mouse xenograft models [5]. Sunitinib exhibits direct antitumor activity by inhibiting RTKs that are expressed by cancer cells and are involved in signaling for cancer cell proliferation [5–12]. Sunitinib also exhibits antiangiogenic activity by inhibition of signaling through vascular endothelial growth factor receptor 2 and platelet-derived growth factor receptor-β RTKs expressed on endothelial cells or stromal cells [6,13].

In a phase 3 multinational study of 750 patients with metastatic RCC, randomized to sunitinib or interferon α (IFNα), the response rate to sunitinib was 31%, with a median progression-free survival (PFS) of 11.7 months and a median survival of 28 months [14]. A recent update of this trial documented an objective response rate of 47% with 11 months of median PFS for sunitinib *versus* 12% objective response rate and 5 months of PFS for IFNα [15]. Although the results with sunitinib therapy are impressive, long-term control of the disease is still not achieved. In addition, several trials documented adverse effects of cardiotoxicity in some of the patients probably as a result of alterations to normal vasculature [16–19]. Therefore, further investigations with sunitinib dose adjustments and combination with other cytotoxic drugs are warranted to decrease the effect on vital organs such as the heart and the kidney.

The process of tumor angiogenesis involves proliferation of abnormal vessels that are enlarged, disorganized, and leaky because of defective basement membrane. These structural defects of tumor vessels cause increased interstitial tissue pressure, impaired blood supply, and decreased oxygen supply in tumors compromising the delivery and efficacy of cytotoxic drugs and radiotherapy [20,21]. To increase the efficacy of chemotherapy, we have recently investigated various doses of sunitinib to cause only partial destruction of immature and inefficient blood vessels leading to "normalization" of tumor vasculature and improve the blood flow in tumors [5]. We used dynamic contrast-enhanced magnetic resonance imaging (DCE-MRI) to image vascular changes induced by sunitinib within the tumor, in an orthotopic KCI-18 model of human RCC xenografts in nude mice. DCE-MRI is a noninvasive approach, currently used in humans, that can detect early changes in the tumor induced by antiangiogenic therapy as reported in human studies [22–25] and in preclinical animal models [26,27]. This method measures a combination of tumor perfusion and vessel permeability and allows the detection of changes in tumor vascularity, which occur at a much earlier stage in the treatment of tumors with antiangiogenic drugs than does shrinkage of tumor mass [23,25].

By assessing vascular changes by DCE-MRI, we showed that a suboptimal daily sunitinib dosage of 20 mg/kg per day mildly affected normal vessels but caused better tumor perfusion and decreased vascular permeability, in agreement with histologic observations of thinning and regularization of tumor vessels [5]. The goals of the current study were to determine whether using sunitinib at doses that regularize the blood flow in the tumor in conjunction with the cytotoxic drug gemcitabine could improve its therapeutic efficacy for RCC. Gemcitabine is a pyrimidine analog that inhibits DNA synthesis. The antitumor activity of gemcitabine depends on a series of sequential phosphorylations leading to accumulation of gemcitabine diphosphate and triphosphate that interfere with DNA elongation by competing with dCTP and also inhibit ribonucleotide reductase, thus reducing the pool of deoxyribonucleotide triphosphates. A few clinical trials have used gemcitabine in combination with other chemotherapy drugs including fluorouracil, thalidomide, and capecitabine or with the cytokine IFNα for metastatic RCC [28–31]. These trials resulted in modest clinical benefit.

Although gemcitabine is a potent antitumor drug, its activity may be reduced by poor access to tumor cells caused by tumor vessel leakiness and increased interstitial tissue pressure [20,21]. In the current study, we have investigated whether improving blood flow by sunitinib, at doses that regularize tumor vessels, could enhance the efficacy of gemcitabine for RCC in murine xenografts kidney tumors. DCE-MRI was used to monitor vascular changes induced by pretreating with sunitinib in KCI-18 kidney tumors to schedule initiation of chemotherapy. We determined the dose and schedule of the combination of antiangiogenic therapy with sunitinib and cytotoxic therapy with gemcitabine that result in significant long-lasting antitumor response. Vascular changes caused by gemcitabine treatment as a single modality or combined with sunitinib were evaluated by DCE-MRI.

Materials and Methods

Orthotopic KCI-18/IK RCC Tumor Model

The human RCC cell line designated KCI-18 was established in our laboratory from a primary renal tumor specimen obtained from a patient with papillary RCC (nuclear grade 3/4) [32]. Cells were cultured in Dulbecco's modified Eagle medium with supplements [32]. After serial passages of KCI-18 cells in the kidney of nude mice, highly tumorigenic KCI-18/IK RCC cell lines were generated [32]. KCI-18/IK cells were washed with Hank's balanced salt solution and subcapsularly injected at a concentration of 5×10^5 cells in 30 μl of Hank's balanced salt solution in the right kidney in 5- to 6-week-old female BALB/C *nu/nu* nude mice (Harlan, Indianapolis, IN) [32]. Mice were housed and handled under sterile conditions in facilities accredited by the American Association for the Accreditation of Laboratory Animal Care. The animal protocol was approved by Wayne State University Animal Investigation Committee.

Experimental Protocol

After injection of KCI-18/IK cells, a few mice were killed at early time points to assess tumor growth before initiating treatment. Small tumors were detectable by days 9 to 10 in the kidney. On day 10, mice bearing established kidney tumors were treated with sunitinib (Pfizer, Inc, New York, NY). The drug was prepared in a carboxymethyl cellulose suspension vehicle, at a dosage of 20 mg/kg per day (SU20) and given orally by gavage [5]. Control mice were treated with vehicle only. After sunitinib pretreatment for 3 days, mice were treated with various doses of gemcitabine administered two to three times a week by intraperitoneal (i.p.) injections. Gemcitabine (Gemzar; Eli Lilly, Indianapolis, IN) was reconstituted in PBS and prepared at doses of 10 to 50 mg/kg. Sunitinib treatment was continued daily for the duration of the experiment. To assess the therapeutic response of kidney tumors to a

combination of sunitinib and gemcitabine, six to eight mice per experimental group were treated. Mice were killed by day 28 after tumor cell injection, when the tumor burden in control animals was large (>1.5 cm × 1 cm in size compared with 0.7 cm × 0.25 cm for normal kidney) compared with the tumor sizes in treated groups [5]. The tumor-bearing right kidneys and the contralateral left normal kidneys were resected and weighed [5]. For survival studies, 12 mice per experimental group were treated with sunitinib at 20 mg/kg per day for 3 days on days 10 to 12 after KCI-18 cell injection in the kidney. Then, mice received five gemcitabine treatments at 20 mg/kg given 3 to 4 days apart, on days 13, 16, 20, 23, and 27. Sunitinib was continued daily for 5 d/wk, for 6 weeks, up to 50 days. Mice were monitored daily for survival, and sick animals were killed and autopsied [33]. On day 50, all remaining mice were killed, and tumor-bearing kidneys were resected and weighed.

Tissue Preparation for Histology

At the completion of experiments, mice were killed, and tumor-bearing kidneys, normal contralateral kidneys, and the lungs were resected and processed for histology. All tissues were fixed in 10% buffered formalin, embedded in paraffin, and sectioned [5]. Sections were stained with hematoxylin-eosin (H&E) [5].

DCE-MRI Monitoring of Tumor Perfusion and Permeability and Tumor Size in Kidney Tumors

On the basis of the initial experiments, early time points between 3 and 11 days after initiation of sunitinib treatment (day 14 through day 21 after tumor cell implantation) were selected for DCE-MRI studies to avoid incorrect analysis of advanced and large necrotic tumors in control mice [5]. Three mice from control-, sunitinib-, and gemcitabine-treated groups were imaged by DCE-MRI. Mice were anesthetized by i.p. injections of 0.35 ml of pentobarbital and 0.35 ml of ketamine at a concentration of 52.5 mg/kg and then a catheter was inserted into their tail vein, which was attached to a syringe containing Gd-DTPA contrast agent (Berlex, Wayne, NJ). Mice were positioned on a cradle heated by temperature-controlled water and were given a second low dose of 15 mg/kg anesthetics (in 0.1 ml volume) to avoid motion problems while in the magnet [5]. A 2-cm-diameter receive-only surface coil was placed over the tumor, and the cradle was placed inside an 11-cm-inner-diameter transmit-only volume coil. DCE-MRI of mice was performed in the MR Research Facility at Wayne State University, using a Bruker Biospec AVANCE animal scanner (Bruker, Karlsruhe, Germany) equipped with a 4.7-T horizontal bore magnet and actively shielded gradients. Anatomic imaging was done using a two-dimensional T2-weighted spin-echo scan (repetition time [TR] = 2000 milliseconds, echo time [TE] = 52.4 milliseconds) to get an overview of the kidney [5]. Baseline imaging data of the kidneys were obtained using the short-TR DCE scan for 30 time points (7 seconds between time points). On time point 10, 100 μl of Gd-DTPA (0.125 mmol/kg) was injected into the tail vein catheter. This dose was selected based on preliminary Gd dose-searching experiments to obtain appropriate contrast for image analysis [5]. Then, imaging data were acquired for 20 more time points. The imaging parameters for this multislice two-dimensional gradient echo scan were as follows: TR = 54.7 milliseconds, TE = 2.9 milliseconds, flip angle = 30°, field of view = 32 mm × 32 mm, slice thickness = 1.5 mm with 0.5 mm gap, matrix size = 128 × 128. Five slices were collected for each animal. Data were processed to determine changes in contrast agent uptake using the SPIN DCE software (Detroit, MI) [34]. For data analysis, the full kidney was selected as the region of interest (ROI) for the tumor-bearing kidney and the contralateral left normal kidney. A threshold was selected to remove noise-only pixels in the image [5]. Gd concentrations [$C(t)$] in the tissue were calculated for all pixels in the ROI and for each time point [34]. Data from the $C(t)$ curves were compiled for each pixel for 16 time points (112 seconds) after Gd injection to create the initial area under the curve (IAUC). The distribution of IAUC for the entire ROI is then shown as a means to visualize the effects in every pixel in a single plot. The CIAUC is the cumulative initial area under the curve of the IAUC histogram [5]. For quantitative analysis of vascular permeability, R_{50} (median) values are derived from CIAUC curves and corresponded to the concentration of Gd at which 50% of the pixels have been included [34]. To evaluate the uptake, washout, and leakage of Gd into the tumor and surrounding kidney tissue, the parametric color maps are used to show the total Gd uptake (AUC) in individual structures. The parameters measured in DCE-MRI for sunitinib- and/or gemcitabine-treated tumors were compared with those obtained for control tumors and normal kidneys.

Analysis of Cell Survival In Vitro by Clonogenic Assay

KCI-18 cells were treated for 24 hours with 1 μM sunitinib or gemcitabine at 1 and 2.5 nM or both drugs combined. Cells were plated in a colony formation assay in triplicate wells of six-well plates at 500 cells per well for control, at 1000 cells per well for sunitinib or gemcitabine alone, and at 3000 cells per well for sunitinib + gemcitabine combined treatment [35]. These plating conditions and drug concentrations were determined based on dose titration experiments. The drugs were added to the cells in the colony plates, and cells were incubated for 10 days at 37°C in a 5% CO_2/5% O_2/90% N_2 incubator. Colonies were fixed, stained, and counted as previously described [35]. The plating efficiency was calculated for each well, and the surviving fraction was normalized to control cells [35].

Statistical Analysis

Evaluation of the shape of the frequency distribution of tumor weights indicated that a log transformation was required to meet the assumptions of normal theory tests. Linear models were used to assess the statistical significance of differences in tumor weight between experimental groups, and proportional hazards models were used for survival data. In both models, indicator variables were used to parameterize dose. Adjustment for multiple comparisons between treatments was made using Holm's procedure to protect against inflated type 1 errors [35,36]. Kaplan-Meier methods were used to graphically compare survival in each of the groups. The log-rank test was used to test differences in survival distributions between groups again using Holm's procedure to control for type 1 error rate.

Results

Direct Cytotoxic Effect of Sunitinib Combined with Gemcitabine in KCI-18 Cells In Vitro

We have previously shown that sunitinib exerts a direct cytotoxic effect on KCI-18 RCC *in vitro*, in a dose-dependent manner [5]. We found that a dose of 1 μM sunitinib caused a significant 40% inhibition in cell survival in a clonogenic assay, as confirmed in this additional experiment (Table 1). This dose was selected to investigate whether this effect is enhanced by the addition of gemcitabine. After

Table 1. Inhibition of KCI-18 Cell Growth by Sunitinib Combined with Gemcitabine *In Vitro*.

Treatment	Survival Fraction (Mean ± SD)	% Inhibition
Control	1.00	0
Gemcitabine (1 nM)	0.52 ± 0.04*	48
Gemcitabine (2.5 nM)	0.21 ± 0.01*	79
Sunitinib (1 μM)	0.64 ± 0.02*	36
Gemcitabine (1 nM) + Sutent (1 nM)	0.19 ± 0.01†	81
Gemcitabine (2.5 nM) + Sutent (2.5 μM)	0.07 ± 0.02†	93

KCI-18 cells were treated with gemcitabine at 1 and 2.5 nM or sunitinib at 1 μM or both drugs in combination for 24 hours, and then cells were plated in a colony formation assay for 10 days. The mean survival fraction was calculated from triplicate wells.
*$P < .001$.
†$P < .0001$.

pilot titration experiments, suboptimal doses of gemcitabine were tested alone and combined with sunitinib in a clonogenic assay. Gemcitabine at doses of 1 and 2.5 μM caused significant inhibition of KCI-18 cell survival of approximately 50% ($P < .001$) and 70% ($P < .0001$), respectively, compared with control cells treated with vehicle (Table 1). This cell growth inhibition was significantly enhanced to 80% and 90% by cotreatment of 1 μM sunitinib with 1 μM and 2.5 μM gemcitabine compared with gemcitabine alone ($P < .01$) and sunitinib alone ($P < .01$) and with control cells ($P < .0001$; Table 1).

Therapeutic Response of Kidney Tumors by Combined Sunitinib and Gemcitabine In Vivo

Using DCE-MRI and histologic studies, we have previously demonstrated that sunitinib, given at a dosage of 20 mg/kg per day for 7 days, caused trimming and regularization of tumor vessels with improved tumor perfusion [5]. This dosage was therefore selected for combination with chemotherapy. To schedule administration of gemcitabine, mice, which had established kidney tumors (mean ± SD; 150 ± 7 mm^3, 186 ± 4 mg) compared with normal kidney sizes (125 ± 2 mm^3, 148 ± 12 mg) on day 10 after tumor implantation, were treated daily with sunitinib at 20 mg/kg per day (SU20) for 3 days and then imaged by DCE-MRI (Figure 1*A*). As observed in our previous studies, the IAUC distribution pattern of Gd uptake and clearance in control mice were different for kidney tumors than for normal kidneys [5]. Slower clearance of Gd was observed in the tumor-bearing kidney compared with faster clearance in the normal kidney, and the CIAUC curve for the tumor-bearing kidney showed a pronounced shift to the right compared with normal kidney, indicative of a greater retention of Gd (Figure 1*A*). In contrast, treatment with SU20 for 3 days showed identical patterns of Gd uptake and clearance in the kidney tumor than in the normal kidney, as previously shown [5]. IAUC and CIAUC histograms of the kidney tumor overlapped those of the normal kidney and shifted to the left compared with control tumor kidneys, indicating decreased Gd retention and improved tumor perfusion (Figure 1*A*). On the basis of these data showing that vascular regularization is detectable by DCE-MRI after 3 days of daily treatment with SU20, we designed the treatment schedule for combination therapy with gemcitabine as presented in Figure 1*B*. Gemcitabine treatment was initiated at 3 days after pretreatment with SU20 for established KCI-18 kidney tumors. The schedule and dose of gemcitabine treatment were determined based on dose titration experiments. After three to five injections of gemcitabine at the dose of 50 mg/kg, given 2 days apart, together with daily SU20, a complete tumor growth inhibition was observed, but this treatment was too toxic to the mice, resulting in 50% death. Therefore, we tested lower doses of 10, 20, and 40 mg/kg of gemcitabine (G10, G20, and G40) given twice a week, 3 days apart, whereas SU20 was continued daily for the duration of the experiment (Figure 1*B*). In separate experimental groups of six to eight mice per group, the response to gemcitabine treatment alone was compared with SU20 alone and both combined in a relatively short-term experiment of 28 days, to compare tumor size at a time point when control tumors are very large. The tumor-bearing right kidney and the normal left kidney were weighed, and the mean tumor weights were compared between each treatment group and control group (Figure 1*C*). After SU20 treatment alone, kidney tumors were significantly smaller by 43% compared with control mice tumors ($P = .001$), but these tumors were still large (Figure 1*C*), as previously reported [5]. Compared with the control, treatment with G10 caused approximately 30% inhibition ($P = .04$) and increased to 52.5% when combined with SU20 ($P < .001$). The effect of G20 was even greater, causing 64% tumor growth inhibition ($P < .001$) and 74% when combined with SU20 ($P < .001$; Figure 1*C*). Although the difference in the mean tumor weight of G20 + SU20 was not significant compared with G20 ($P = .33$), the tumor weight data ($n = 8$) in the combined treatment were more consistent and less variable than with G20 only. The mean weight of tumor-bearing kidneys of mice treated with SU20 + G20 was only 223 ± 37 mg, and their shape and size consistently looked closer to those of normal kidneys (166 ± 22 mg) with a mean difference of only 57 mg (Figure 1*C*). This combined therapy using 20 mg/kg per day of sunitinib combined with four treatments of gemcitabine at 20 mg/kg given 3 days apart for a total of 80 mg/kg did not cause any signs of toxicity to the mice. However, when the dose of gemcitabine was increased to 40 mg/kg, for a total of 160 mg alone or together with SU20, it was associated with toxicity and weight loss. Treatment with G40 resulted in significant tumor growth inhibition of 71% ($P < .001$) when given alone, but no further increase was observed with combination with SU20 compared with G40 alone ($P = .53$; Figure 1*C*). The difference between the G20 and G40 groups was not statistically significant ($P = .51$). It should be noted that the size of the normal contralateral kidneys was not affected by the single or combined therapy at every dose of gemcitabine tested (Figure 1*C*, *inset*).

Survival of Kidney Tumor–Bearing Mice Treated with Combined Sunitinib and Gemcitabine

From the experiments presented in Figure 1, we have determined the sequence, schedule, and doses for a safe and therapeutic combination of sunitinib and gemcitabine for treating KCI-18 kidney tumor–bearing mice. We showed that a dosage of sunitinib of 20 mg/kg per day combined with gemcitabine at 20 mg/kg per treatment for four treatments results in optimal and consistent tumor growth inhibition, when this effect was assessed on day 28 after tumor implantation (Figure 1*C*). These conditions were selected to evaluate the effect of single and combined therapies on mouse survival during a longer-term experiment of 50 days. Mice bearing established kidney tumors were pretreated with 20 mg/kg per day sunitinib for 3 days (days 10-12) followed by four injections of gemcitabine at 20 mg/kg given 3 days apart (days 13, 16, 20, and 23) following the same schedule shown in Figure 1*B*. An additional gemcitabine injection was administered on day 23 because of the longer duration of the experiment.

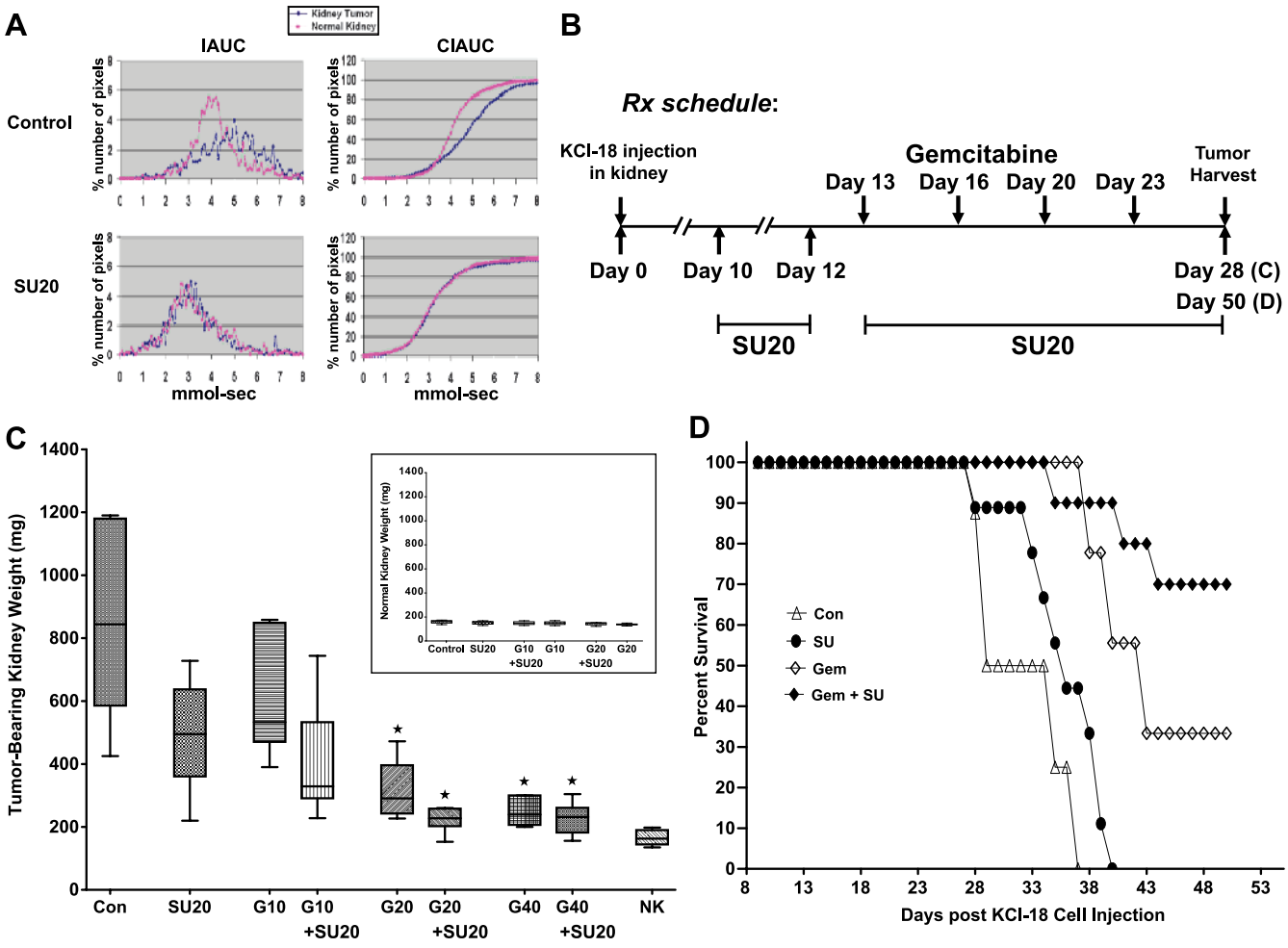

Figure 1. KCl-18 kidney tumor response to sunitinib combined with gemcitabine. (A) DCE-MRI of early vascular changes induced by sunitinib. Mice bearing established kidney tumors were treated daily with sunitinib at 20 mg/kg per day (SU20) for 3 days and imaged by DCE-MRI. (B) Treatment schedule for combination therapy. Mice bearing established kidney tumors were pretreated with sunitinib at 20 mg/kg per day (SU20) for 3 days on days 10 to 12 after KCl-18 cell injection in the kidney. Then, mice received gemcitabine treatments at 10, 20, or 40 mg/kg given 3 days apart, twice a week for 2 weeks on days 13, 16, 20, and 23. Sunitinib was continued daily for up to 28 days for a short-term experiment (C) or for 50 days for a longer-term experiment (D). (C) Response of tumor-bearing kidneys to single and combined therapy. On day 28, tumor-bearing kidneys and contralateral normal kidneys were resected and weighed. The weights of the tumor-bearing kidneys and their median are reported for six to eight mice per group treated with vehicle (control) or sunitinib at 20 mg/kg per day (SU20) or gemcitabine at 10 (G10), 20 (G20), or 40 mg/kg (G40); each drug alone and in combination compared with the normal contralateral kidney weights (NK). Inset shows weights of the normal contralateral kidneys for each treatment group. *$P <$ .001. (D) Survival of KCl-18 kidney tumor–bearing mice treated with sunitinib combined with gemcitabine. Mice bearing established kidney tumors were pretreated with sunitinib (SU) at 20 mg/kg per day for 3 days on days 10 to 12 after KCl-18 cell injection in the kidney. Then, mice received five gemcitabine (Gem) treatments at 20 mg/kg given 3 to 4 days apart, during 3 weeks on days 13, 16, 20, 23, and 27, and sunitinib was continued daily, 5 days per week, for up to 50 days as shown in Figure 2*B*. Mice were followed for survival and Kaplan-Meier survival curves of mice treated with vehicle (Con for control) sunitinib (SU) or gemcitabine (Gem) or both combined (Gem + SU) were constructed.

Sunitinib was continued daily for 5 d/wk for 6 weeks, up to day 50 (Figure 1*B*). Mice were monitored on a daily basis; sick mice showing weight loss and/or limited mobility, as a result of large kidney tumors, were killed and necropsied; and the tumor weights were measured. Survival of animals receiving sunitinib alone was not statistically different from control mice (P = .08; median SU = 36 days; median controls = 29 days; Figure 1*D*). In both groups, mice had large kidney tumors at necropsy, the mean tumor weights of control mice was 1157 ± 426 mg, and that of sunitinib treated mice was 675 ± 226 mg. Animals treated with gemcitabine alone for a total dose of 100 mg/kg had a median survival of 43 days, significantly longer survival than controls ($P <$ .001) and than the sunitinib group (P = .009), but only 33% of the mice survived up to day 50. These mice had large tumors with mean weight of 794 ± 338 mg when necropsied. The combination of sunitinib and gemcitabine resulted in longer survival compared with control mice ($P <$ .001) and mice treated with sunitinib ($P <$ .001) but was not significantly different from animals treated with gemcitabine alone (P = .13; Figure 1*D*). Nevertheless, a higher proportion of 70% of the mice (7/10) treated with the combined therapy survived by day 50 compared with 33% with gemcitabine alone and 0% with sunitinib alone. Interestingly, these mice had large tumors with a mean of 767 ± 267 mg, probably because of the regrowth of kidney tumors, which

was not controlled by maintenance therapy with sunitinib at 20 mg/kg per day.

In Situ Effects of Sunitinib and Gemcitabine on Kidney Tumors and Lung Metastases

Tumor-bearing kidneys and normal contralateral kidneys from mice treated with sunitinib at 20 mg/kg per day, gemcitabine at 20 mg/kg, and both combined were obtained on day 28 from experiments described in Figure 1, *B* and *C*. These tissues were processed for histology and H&E staining. Kidney tumors from control mice presented as a high-grade carcinoma, consisting of tumor cells with large pleomorphic nuclei, prominent nucleoli, abundant eosinophilic cytoplasm, and large cytoplasmic inclusions [5,32]. These tumors were highly vascularized with a sinusoidal vascular pattern consisting of abnormal enlarged vessels (Figure 2*A*). Focal extravasation of red blood cells (RBCs) between tumor cells was observed probably because of the leakiness of vessels and disrupted basement membrane as previously reported [5,32]. Kidney tumors treated with sunitinib showed considerable thinning, regularization, and organization of tumor vessels with endothelial cells lining the vessels (Figure 2*A*). A marked decrease in the number of tumor vessels was noted (Figure 2*A*). These findings are consistent with our previous observations [5]. Kidney tumors of mice treated with gemcitabine showed abnormal giant tumor cells exhibiting degenerative changes in their cytoplasm and nuclei, which were indicative of cell death (Figure 2*A*). These giant cells, comprising approximately 70% of the tumor, contained cytoplasmic vacuoles and pink eosinophilic inclusions and showed degenerative changes in nuclei with focal karyopyknosis (Figure 2*A*). Compared with control tumors, the vascularity of these gemcitabine-treated tumors was reduced and had lower numbers of enlarged vessels. A few focal enlarged vessels were still observed along with few foci of RBC's extravasation (Figure 2*A*). Kidney tumors treated with sunitinib and gemcitabine showed a higher frequency of approximately 90% abnormal giant tumor cells harboring the same cytoplasmic and nucleus degenerative changes as those seen in gemcitabine alone (Figure 2*A*). The tumor vessels looked more trimmed and more organized than those seen after gemcitabine treatment alone, although focal dilatation was still observed compared with sunitinib-treated tumors. In lower magnifications, these tumors looked like residual small nodules mostly consisting of giant tumor cells, which were surrounded by normal epithelial renal cells (data not shown). The histologic diagnosis of tumors treated with 40 mg/kg of gemcitabine alone or with sunitinib was comparable to that shown in Figure 2*A* for tumors treated with 20 mg/kg gemcitabine.

Tissue sections from the normal contralateral left kidneys (not implanted with tumor) were also evaluated after single and combined sunitinib and gemcitabine treatments (Figure 2*B*). Normal kidneys from untreated control mice showed preserved kidney tissue architecture with intact and regular blood vessels. As observed previously, sunitinib at 20 mg/kg per day caused mild dilatation of a few vessels [5]. Interestingly, gemcitabine caused dilatation of some of the vessels and mild focal extravasation of RBCs (Figure 2*B*). After combined sunitinib and gemcitabine treatment, focal areas of dilated vessels were seen but at a lower frequency than with gemcitabine alone (Figure 2*B*).

Spontaneous metastasis to the lungs from primary KCI-18 kidney tumors has been previously observed in this RCC metastatic model [32]. To assess the effect of therapy on spontaneous lung metastases, lungs were resected on day 28 from kidney tumor–bearing mice treated with sunitinib and gemcitabine and processed for H&E staining. In control kidney tumor–bearing mice, all mice presented with metastatic lung tumor nodules showing the typical morphology of KCI-18 RCC tumor cells with large pleomorphic nuclei and prominent nucleoli (Figure 3). Areas of dilated vessels with extravasation of RBCs were observed as seen in primary kidney tumors (Figure 3). The average number of lung nodules was 26 per mouse consisting of a mixture of large and small nodules. In sunitinib-treated mice, all mice had metastatic lung nodules, but most of the nodules were very small, often containing less than 10 cells per nodule and an average of 14 per mouse. The lung tumor nodules showed an overall decrease in the number of tumor cells and/or areas of tumor destruction as well as a marked decrease in vascularization (Figure 3). Mice treated with 20 or 40 mg of gemcitabine had a lower frequency of lung nodules detectable in three of seven mice and presenting as one to five small lung nodules per mouse. These lung tumor nodules exhibited giant tumor cells with cytoplasmic vacuoles, eosinophilic inclusions, and degenerative nuclei identical to those observed in primary kidney tumors treated with gemcitabine (Figure 3). Few trimmed vessels were seen. The effect of combined sunitinib and gemcitabine on metastatic lung nodules was more drastic with large areas of hyalinization and fibrosis and few remaining giant tumor cells with degenerative changes (Figure 3). Lung tumor nodules were detectable only in 3 of 11 mice treated with sunitinib combined with 20 or 40 mg/kg gemcitabine, and most of these nodules were very small, often containing less than five cells per nodule and large areas of fibrosis.

DCE-MRI Evaluation of Vascular Changes Induced by Gemcitabine Treatment in Kidney Tumors

To monitor the effect of gemcitabine treatment by DCE-MRI, mice with established kidney tumors were treated on day 13 with gemcitabine at a safe and therapeutic dose of 20 mg/kg, given 3 to 4 days apart, as determined from experiments described in Figure 1. Mice were then tested by DCE-MRI after one, three, or four doses of gemcitabine (days 14, 18, and 21, respectively). For data analysis, the full kidney was selected as the ROI for both right tumor-bearing kidney and left normal kidney (Figure 4*A*). As described previously in Figure 1*A*, the IAUC and CIAUC curves for the tumor-bearing kidney in control mice showed a pronounced shift to the right compared with normal kidney, indicative of a greater retention of Gd (Figure 4, *B-D*). Interestingly, gemcitabine treatment caused improved clearance of Gd in the tumor-bearing kidney compared with kidney tumors from control mice (Figure 4*B*). This was observed by a shift of the IAUC and CIAUC curves toward those of normal kidneys (Figure 4, *C* and *D*). Furthermore, the patterns of Gd uptake and clearance were identical in the tumor-bearing kidney and the normal kidney with IAUC and CIAUC curves overlapping and thus indicative of improved blood perfusion in the tumor (Figure 4). Gemcitabine also changed the pattern of uptake and clearance in the normal kidney compared with the normal kidney of control mice, showing a slower washout of Gd (Figure 4*B*) and a wider IAUC distribution (Figure 4*C*). These data suggest that gemcitabine is also causing vascular changes in the normal kidney. It should be noted that vascular changes both in the kidney tumors and in normal kidneys are consistently observed with one, three, or four doses of gemcitabine. These findings suggest that one dose of gemcitabine is sufficient to induce vascular changes that are reproducible with additional treatments of gemcitabine.

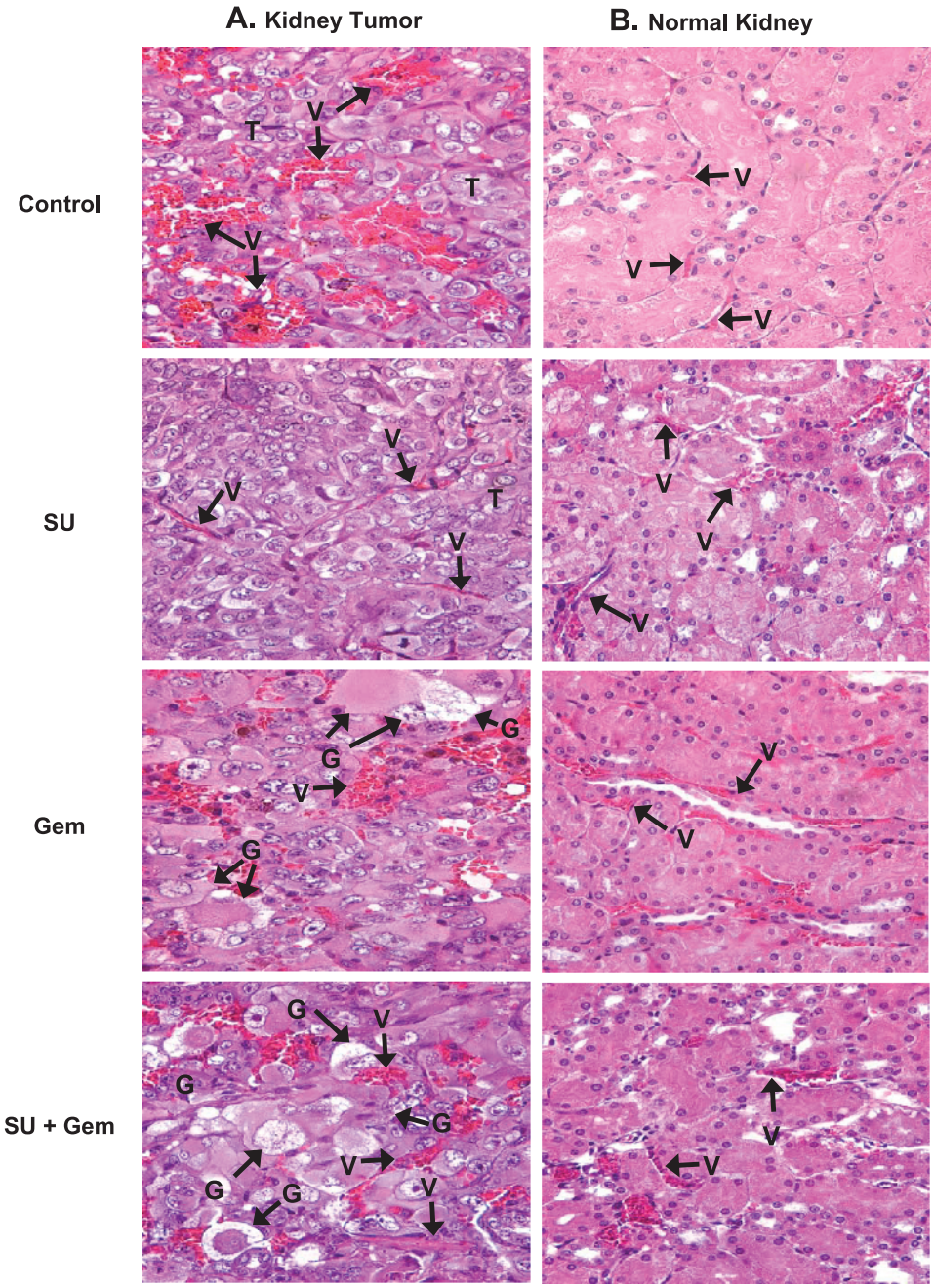

Figure 2. Histology of kidney tumors and normal kidneys from mice treated with sunitinib and gemcitabine. Kidney tumors and normal contralateral kidneys from mice treated with sunitinib (20 mg/kg), gemcitabine (20 mg/kg), and both combined, obtained on day 28 from experiments described in Figure 1, were processed for histology and H&E staining. The main findings were labeled on the prints with T for tumor, V for vessels, G for giant tumor cells. (A) Kidney tumors. Control untreated tumors consisted of tumor cells with large pleomorphic nuclei were highly vascularized with a sinusoidal vascular pattern of abnormal enlarged dilated vessels with focal extravasation of RBCs. Sunitinib (SU)-treated tumors showed thinning and organization of tumor vessels as well as a decrease in the numbers of tumor vessels. Kidney tumors of mice treated with gemcitabine (Gem) contain numerous abnormal and giant tumor cells with cytoplasmic vacuoles or eosinophilic inclusions and degenerative changes in nuclei with focal karyopyknosis. Note some of the vessels in these tumors were still enlarged with foci of RBCs extravasation, however, to a lesser degree than in the untreated tumors. Tumors treated with sunitinib and gemcitabine (SU + Gem) consisted mostly of abnormal degenerating giant tumor cells. Trimming of tumor vessels was evident. (B) Normal contralateral left kidneys. The normal kidney from control mice showed intact, regular, and thin blood vessels. Sunitinib at 20 mg/kg showed a mild effect of dilatation in a few vessels. Gemcitabine caused dilatation of some of the blood vessels. This effect was milder with combined sunitinib and gemcitabine with fewer vessels dilated. All magnifications, ×40.

DCE-MRI parametric maps were derived from the $C(t)$ curves for each pixel and represent the total Gd uptake (AUC) for the tumor and surrounding kidney tissue (Figure 4*E*). Parametric maps from control mice showed accumulation of Gd in the periphery of the tumor with no uptake in the tumor core, indicative of poor tumor perfusion (Figure 4*E*), as previously reported [5]. In the normal kidney of control mice, Gd uptake was distributed in the entire kidney with a higher uptake in the medullary central area than in the peripheral cortex, probably reflecting normal secretion of contrast agent (Figure 4*E*). Interestingly, gemcitabine caused striking changes observed by parametric maps with uptake of Gd in the core of the tumor, indicative of tumor perfusion (Figure 4*E*). The uptake of Gd in the tumor-bearing kidney was similar to that seen in the normal kidney (Figure 4*E*). These data were consistently reproduced after one, three, or four treatments of gemcitabine injections (Figure 4*E*).

DCE-MRI of Kidney Tumors Treated with Sunitinib and Gemcitabine

The effect of sunitinib, gemcitabine and both combined on kinetics of Gd uptake and clearance in tumors was evaluated by DCE-MRI. In this experiment, KCI-18 kidney tumor–bearing mice were pretreated daily with sunitinib at a dose of 20 mg/kg per day (SU20), for 3 days on days 10, 11, and 12 after KCI-18 cell implantation in the right kidney. On day 13, gemcitabine (GEM) was injected i.p. at 20 mg/kg, and this injection was repeated on days 15 and 17 while continuing daily treatment with SU20. After these three doses of gemcitabine, on day 18, mice were imaged by DCE-MRI as previously described [5]. For data analysis, the full kidney was selected as the ROI for both right tumor-bearing kidney and left normal kidney (Figure 5*A*). Analysis of the kinetics of uptake and clearance of Gd showed that in control mice, the clearance of Gd in the tumor-bearing kidney was slow compared with faster clearance in the normal kidney (Figure 5, *B-D*). After treatment with SU20, the $C(t)$ curves of the kidney tumors overlapped those of normal kidneys and showed similar uptake and improved Gd clearance with much less Gd retention than that of kidney tumors in control mice (Figure 5*B*). The tumor-bearing kidney IAUC curve looked more regular and shifted to the left compared with control kidney tumors indicating decreased Gd retention (Figure 5*C*). Gd uptake and clearance in the $C(t)$ curves, IAUC and CIAUC showed identical patterns in the tumor-bearing kidney compared with the normal kidney (Figure 5, *B-D*). These findings are consistent with our previous studies [5] and suggest a return to more "normal vasculature" with lower permeability (i.e., less leaky vessels). After treatment with gemcitabine, the vascular changes described in Figure 4 were reproduced in this experiment, including

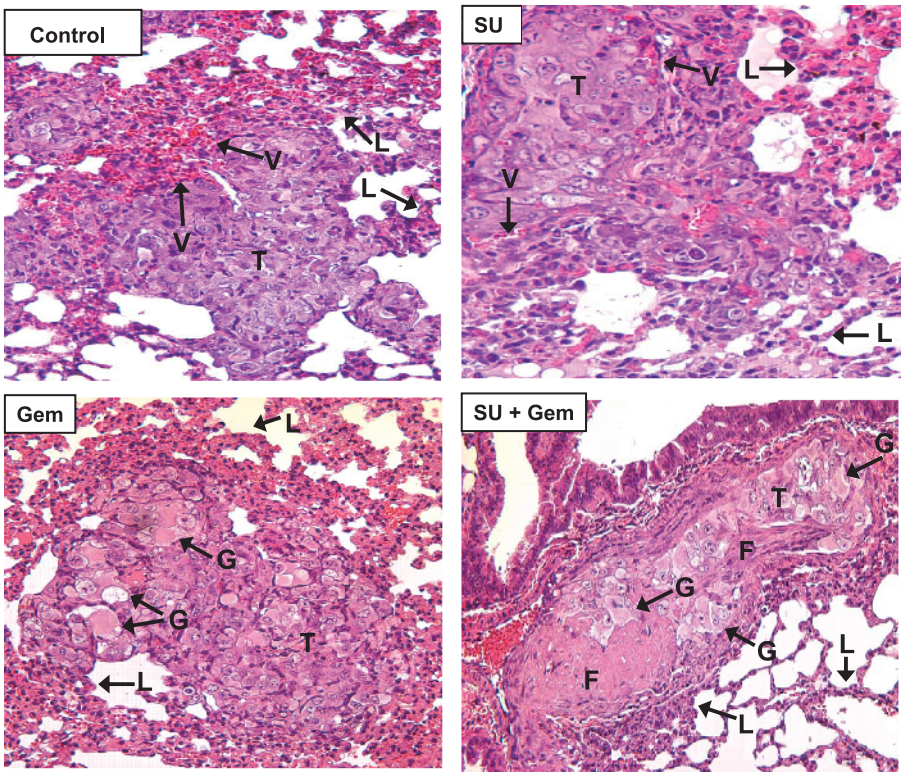

Figure 3. Histology of spontaneous lung metastases from mice treated with sunitinib and gemcitabine. Lungs from mice treated with sunitinib (20 mg/kg), gemcitabine (20 mg/kg), and both combined, obtained on day 28 from experiments described in Figure 1, were processed for histology and H&E staining. The main findings were labeled on the prints with T for tumor, V for vessels, G for giant tumor cells, F for fibrotic areas, and L for normal lung alveoli. Metastastic lung tumor nodules from untreated mice (Control) consisted of tumor cells with pleomorphic nuclei and prominent nucleoli and contained areas of dilated vessels. Sunitinib (SU)-treated mice had decreased number of tumor cells and vessels in lung tumor nodules. Lung tumor nodules from gemcitabine (Gem)- treated mice showed giant tumor cells with cytoplasmic vacuoles and eosinophilic inclusions and decreased vascularization. Gemcitabine combined with sunitinib (SU + Gem) contained large eosinophilic areas of hyalinization, fibrosis, and a few giant abnormal tumor cells. Figures were enlarged to show changes in lung tumor nodules.

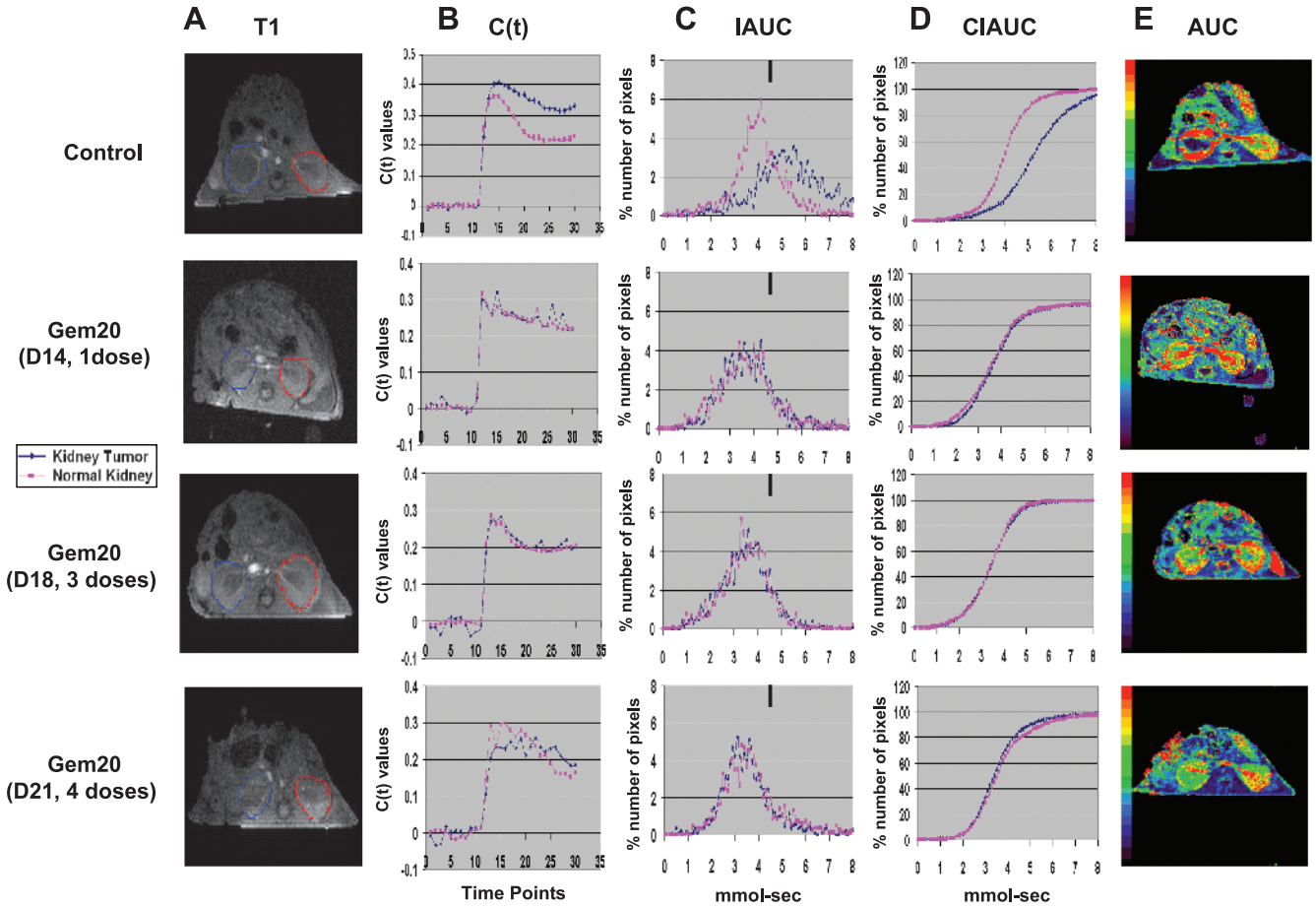

Figure 4. DCE-MRI imaging of vascular changes induced by gemcitabine in KCI-18 kidney tumors. In separate experiments, mice bearing established kidney tumors were treated with gemcitabine at 20 mg/kg (Gem20) or with vehicle (control). Mice were imaged by DCE-MRI at 24 hours after gemcitabine treatment after receiving one dose (day 14), three doses (day 18), or four doses (day 21), given 3 days apart. (A) T1 images: Baseline images before Gd contrast agent injection. The full kidney was selected as the ROI for the tumor-bearing kidney (blue contour on left of T1 image) and the contralateral normal kidney (red contour on right of T1 image). (B) $C(t)$ kinetics of Gd contrast uptake and clearance: The first 10 time points represent baseline data. Gd was injected at time point 10, and images were collected for 20 more time points. (C) IAUC graphs: Data from the $C(t)$ curves were compiled for 16 time points (112 seconds) after Gd injection to draw $IAUC_{112}$. The small black bar indicates the peak position of normal kidney in control mice and can be used as a reference for curve shifting in normal kidneys and kidney tumors treated with gemcitabine. (D) CIAUC graphs: CIAUC curves were derived from IAUC curves. In panels A, B, C, and D, blue lines are for kidney tumors and pink lines are for normal kidneys. (E) AUC parametric map: Parametric color maps were constructed based on uptake and concentration of Gd in the tissue, represented by the colors blue, green, yellow, and red with gradual increase of Gd from lowest values (blue) to highest values (red). The tumor-bearing kidney is on the left, and the normal contralateral kidney is on the right of the MR images. The color coding in the kidneys are shown for integrated AUC. Data from a representative mouse from each treatment group are presented.

improved clearance of Gd in the tumor-bearing kidney and slower clearance of Gd in the normal kidney (Figure 5, *B-D*). After combined therapy of SU20 with gemcitabine, the patterns of Gd uptake and clearance resembled those of gemcitabine alone both in kidney tumors and normal kidneys with a tendency to decreased clearance of Gd (Figure 5, *B-D*). As observed for SU20 alone, the IAUC and CIAUC curves of kidney tumor and normal kidney overlapped and showed a pattern close to that of normal kidney in control mice (Figure 5, *C* and *D*).

DCE-MRI parametric maps were derived from the $C(t)$ curves for each pixel and represent the total Gd uptake (AUC) for the tumor and surrounding kidney tissue (Figure 5*E*). As described for Figure 4, parametric maps from control mice consistently showed accumulation of Gd in the periphery of the tumor with no uptake in the tumor core, indicative of poor tumor perfusion (Figure 5*E*). Parametric maps of SU20-treated mice showed a significant accumulation of Gd in the tumor-bearing kidney including Gd uptake in the tumor and also Gd accumulation in the normal kidney (Figure 5*E*), as shown previously [5]. Gemcitabine caused striking changes observed by parametric maps with tumor perfusion and an uptake of Gd similar to normal kidney (Figure 5*E*), as shown in separate experiments in Figure 4*E*. These findings were reproduced with the combined SU20 and gemcitabine including tumor perfusion but less Gd accumulation than that seen with SU20 alone (Figure 5*E*).

DCE-MRI Quantitation of Vascular Changes of Kidney Tumors Treated with Sunitinib and Gemcitabine

To quantitate the vascular changes induced by sunitinib and gemcitabine and study the reproducibility of our findings, R_{50} values for five mice per treatment group were derived from CIAUC curves for

both kidney tumors and normal kidneys [5]. The R_{50} (median) values correspond to the concentration of Gd at which 50% of the pixels have been included (Figure 6*A*) [5,34]. Lower R_{50} values were consistently observed in mice treated with SU20, gemcitabine, and both combined compared with control mice for kidney tumors (Figure 6*B*). Compared with R_{50} values of normal kidneys in control mice, a trend to lower R_{50} was also observed for normal kidneys suggesting a mild systemic effect of both drugs affecting blood flow (Figure 6*C*). To compare the vascular changes induced by the drugs in kidney tumors to those induced in normal kidneys, R_{50} values of kidney tumors were normalized to the R_{50} values of normal contralateral kidneys for each mouse (NR_{50} KT *vs* NK; Figure 6*D*) [5]. These values were consistently much smaller in mice treated with each drug and both combined compared with control mice (Figure 6*D*). Normalization of R_{50} values of treated kidney tumors *versus* control kidney tumors (NR_{50} KT_{treat} *vs* KT_{cont}) showed negative values with each drug alone and both combined (Figure 6*E*). To assess the effect of SU20 and gemcitabine on normal contralateral kidneys, R_{50} values of normal kidneys from treated mice were normalized to normal kidneys from control mice (Figure 6*F*). These NR_{50} data of normal kidneys showed also negative values for mice treated with each drug separately and both combined (Figure 6*F*) but less than

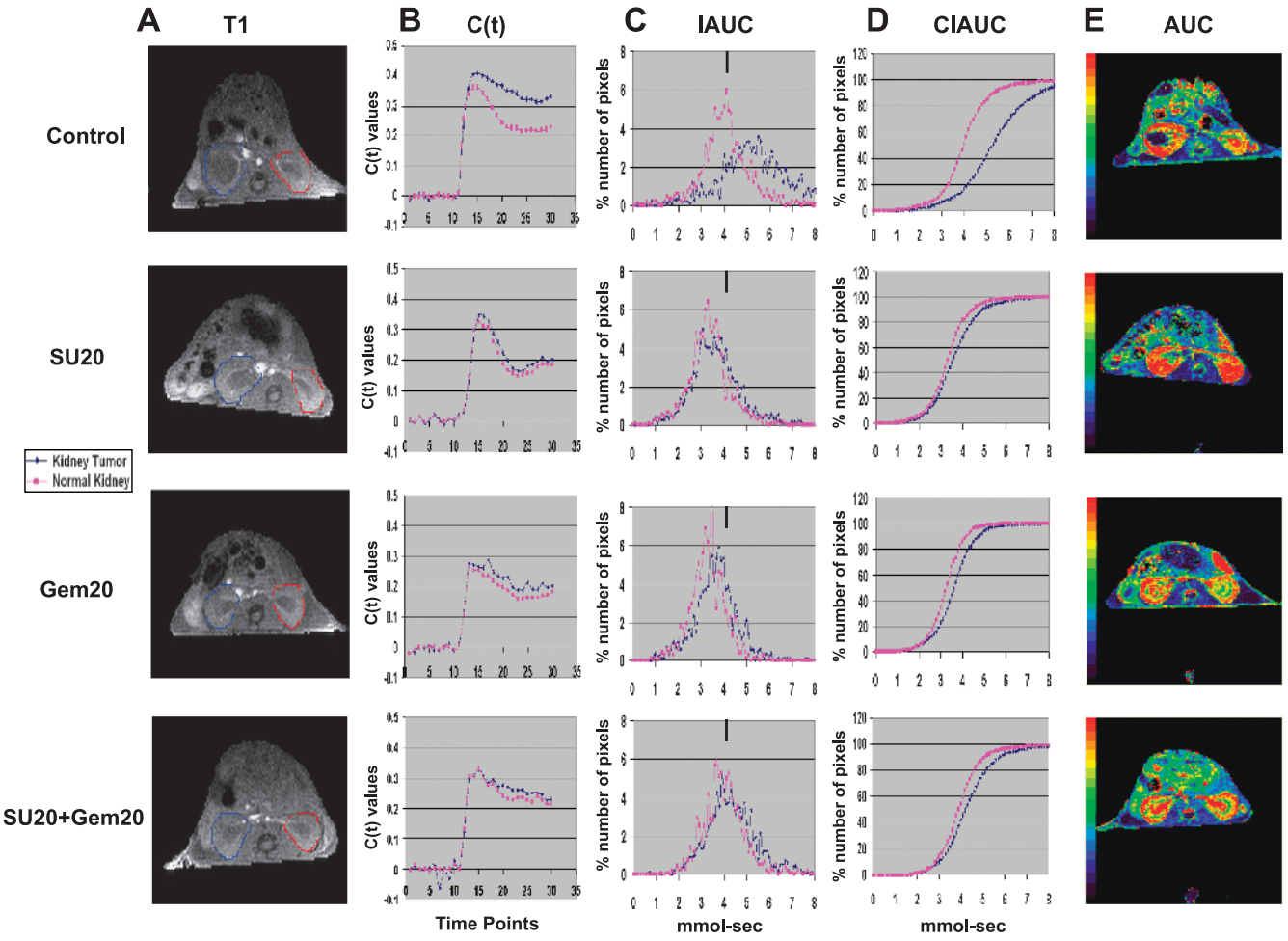

Figure 5. DCE-MRI imaging of vascular changes induced by gemcitabine and sunitinib in KCI-18 kidney tumors. Separate experimental groups of three mice per group were treated with vehicle only (control), sunitinib only (SU20), gemcitabine only (Gem20), or sunitinib + gemcitabine (SU20 + Gem20). Mice bearing established kidney tumors were pretreated with sunitinib at 20 mg/kg per day (SU20) for 3 days on days 10 to 12 after KCI-18 cell injection in the kidney. Then, mice received three gemcitabine treatments at 20 mg/kg (Gem20) given on days 13, 15, and 17 while continuing daily sunitinib treatments. At 24 hours after the last gemcitabine treatment (day 18), mice were imaged by DCE-MRI for 30 time points at 7-second intervals. (A) T1 images: Baseline images before Gd contrast agent injection. The full kidney was selected as the ROI for the tumor-bearing kidney (blue contour on left of T1 image) and the contralateral normal kidney (red contour on right of T1 image). (B) *C*(*t*) kinetics of Gd contrast uptake and clearance: The first 10 time points represent baseline data. Gd was injected at time point 10, and images were collected for 20 more time points. (C) IAUC graphs: Data from the *C*(*t*) curves were compiled for 16 time points (112 seconds) after Gd injection to draw $IAUC_{112}$. The small black bar indicates the peak position of normal kidney in control mice and can be used as a reference for curve shifting in normal kidneys and kidney tumors after treatment. (D) CIAUC graphs: CIAUC graphs were derived from IAUC curves. In graphs B, C, and D, blue lines are for kidney tumors and pink lines are for normal kidneys. Data from a representative mouse from each treatment group are presented. (E) AUC parametric map: Parametric color maps were constructed based on uptake and concentration of Gd in the tissue, represented by the colors blue, green, yellow, and red with gradual increase of Gd from lowest values (blue) to highest values (red). The tumor-bearing kidney is on the left, and the normal contralateral kidney is on the right of the MR images. The color coding in the kidneys are shown for integrated AUC.

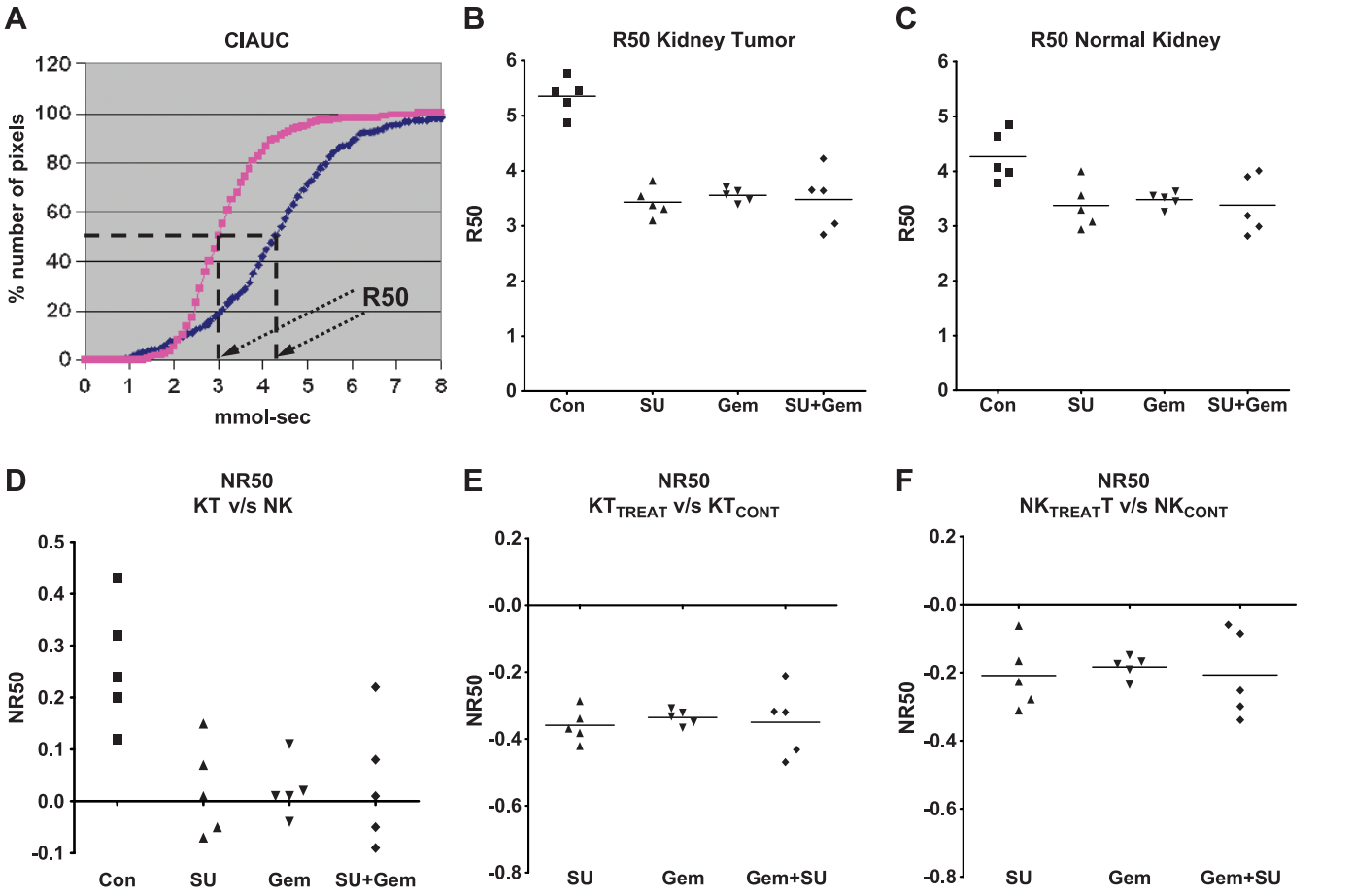

Figure 6. R_{50} quantitation of DCE-MRI data of KCI-18 kidney tumors. Mice were treated with vehicle (control, Con), sunitinib at 20 mg/kg per day (SU), gemcitabine at 20 mg/kg (Gem), or both sunitinib and gemcitabine and were then imaged by DCE-MRI as described in Figure 5. Data obtained from MR images were quantitated. (A) R_{50} value calculation: The R_{50} value is derived from CIAUC curves (as shown for control mouse) and corresponds to the Gd concentration at which 50% of the pixels have been included. (B) Tumor-bearing kidney R_{50}: R_{50} of kidney tumors from five mice per treatment group. (C) Normal kidney R_{50}: R_{50} normal contralateral kidney for each mouse shown in B. (D) NR_{50} of KT *versus* NK: NR_{50} represents normalization of R_{50} values of kidney tumors (KT) relative to R_{50} values of normal contralateral kidney (NK) calculated as $[R_{50KT} - R_{50NK}] / R_{50NK}$ for each mouse. (E) NR_{50} of KT_{TREAT} *versus* KT_{CONT}: Normalization of R_{50} values of kidney tumors from treated mice (KT_{TREAT}) relative to the mean R_{50} values of kidney tumors from control mice (KT_{CONT}) calculated as $[R_{50}\ KT_{TREAT} - R_{50}\ KT_{mean\ cont}] / R_{50}\ KT_{mean\ cont}$ for each mouse. (F) NR_{50} of NK_{TREAT} *versus* NK_{CONT}: Normalization of R_{50} values of normal kidneys of treated mice relative to the mean R_{50} values of normal kidneys from control mice calculated as $[R_{50}\ NK_{TREAT} - R_{50}\ NK_{mean\ cont}] / R_{50}\ NK_{mean\ cont}$ for each mouse. Data are presented for five mice per treatment group in each panel.

those of NR_{50} KT_{treat} *versus* KT_{cont}. These data indicate a relatively mild effect by either drug alone and combined on normal kidney vasculature (Figure 6*F*) in contrast to a more pronounced effect on vasculature of kidney tumors (Figure 6*E*).

Discussion

The concept of normalization of tumor vessel through elimination of excess endothelial cells to improve the blood flow, reduce vessel leakiness and interstitial pressure, and increase drug delivery to tumor cells has shown promise for combination with anticancer drugs [37–39]. We have previously determined the doses and schedule of the antiangiogenic drug sunitinib that cause thinning and regularization of tumor vessels in kidney tumors of the KCI-18 RCC orthotopic tumor model in nude mice [5]. We found that daily treatment with 20 mg/kg per day of sunitinib caused better tumor perfusion and decreased vascular permeability by DCE-MRI [5]. These observations on vascular changes were in agreement with *in situ* histologic studies demonstrating thinning and regularization of tumor vessels [5]. In addition, this dose caused only mild changes in vessels in normal kidney tissue and was not toxic to the mice [5]. On the basis of these findings, the dosage of 20 mg/kg per day of sunitinib was selected to regularize the blood flow in the tumor and then schedule chemotherapy with gemcitabine. The conditions for combining antiangiogenic therapy with chemotherapy were investigated.

Dose-searching studies using 10, 20, or 40 mg/kg of gemcitabine showed that a schedule of injections given 3 days apart was less toxic than every 2 days. Doses of 20 and 40 mg/kg gemcitabine were more effective than 10 mg/kg and caused significant kidney tumor growth inhibition. To schedule the combination of gemcitabine with sunitinib, regularization of tumor vessels was monitored by DCE-MRI of kidney tumor–bearing mice treated with sunitinib only. DCE-MRI showed that 1 day of sunitinib treatment at a dosage of 20 mg/kg per day was not sufficient to induce regularization of vasculature and resulted

only in minor vascular changes (G.G.H., unpublished data, 2010). However, DCE-MRI of mice treated for 3 days with 20 mg/kg per day sunitinib confirmed that this schedule was sufficient to induce vascular changes of decreased Gd retention and improved tumor perfusion in KCI-18 kidney tumors, indicating normalization of blood vessels. Therefore, gemcitabine treatment was initiated after three consecutive daily treatments of sunitinib. When gemcitabine was administered after sunitinib and given at a dose of 20 mg/kg for four treatments, whereas continuing daily administration of sunitinib, the effect of the combined therapy was particularly effective causing approximately 74% reduction in tumor weight by day 28. This schedule and dosage of sunitinib given in conjunction with gemcitabine were well tolerated by the mice and were not associated with toxicity. This combined therapy significantly inhibited the growth of the tumor in the kidney, and this effect was consistent in all mice tested in contrast to greater variability from mouse to mouse with each modality alone. The size and shape of the tumor-bearing kidneys were comparable to those of the normal contralateral kidneys. In agreement with our gross observations, only small residual tumor nodules surrounded by normal kidney tissue were histologically observed. Tumors treated with gemcitabine alone or both gemcitabine and sunitinib showed a high frequency of abnormal giant tumor cells with degenerative changes in their cytoplasm and nuclei, indicative of processes of cell death. Similar effects of the single and combined modalities were also observed histologically in the spontaneous lung metastases. In lungs of sunitinib-treated mice, the tumor nodules showed a decrease in size, cellularity, and vascularization, probably as a result of the antiangiogenic activity of sunitinib. Gemcitabine treatment caused a marked increase in giant tumor cells with degenerative processes in metastatic lung nodules, which looked identical to those observed in primary kidney tumors. This effect was more pronounced in lung tumor nodules treated with the combined therapy, as visualized by few remaining giant tumor cells surrounded by fibrotic areas. The frequency and size of metastatic lung tumor nodules were drastically reduced by gemcitabine alone or combined with sunitinib compared with control mice. These findings observed in spontaneous lung metastases suggest that sunitinib and gemcitabine act systemically affecting both the primary and metastatic tumors, and therefore, a combined approach of antiangiogenic drug and chemotherapy drug could be effective for metastatic RCC disease.

Long-term survival studies, using a schedule of 3 days of 20 mg/kg of sunitinib followed by five treatments of 20 mg/kg of gemcitabine and continued daily administration of sunitinib resulted in a significant increase in mouse survival. Interestingly, although sunitinib daily treatment was continued after gemcitabine therapy, kidney tumors recurred as observed by day 50. These data suggest that 20 mg/kg of sunitinib was not sufficient to maintain the initial dramatic inhibition of tumor growth induced by gemcitabine and prevent regrowth of tumor vessels. It should be noted that the total dose of gemcitabine (100-120 mg/kg) used in our study is much lower than that used in pancreatic cancer preclinical models (480 mg/kg) [40]. This low dose of gemcitabine in our RCC preclinical model is very effective when combined with an antiangiogenic drug as shown in the pancreatic cancer model [40]. These data also demonstrate that DCE-MRI is a useful means to monitor early vascular changes induced by sunitinib to assess improved blood flow and schedule initiation of chemotherapy. Recent clinical studies have successfully shown that early changes in DCE-MRI of cancer patients have the potential to predict response and guide therapy [41–43].

Our previous observations of uptake and clearance of Gd in control kidney tumors monitored by DCE-MRI were confirmed in the current study [5]. These patterns included slow clearance of Gd and accumulation of Gd in the periphery of the tumor with no uptake in the tumor core, as seen in parametric maps. These findings suggested poor tumor perfusion, probably as a result of leakiness from abnormal enlarged tumor vessels as observed by histology of tumor sections and extravasation of RBCs [5]. Imaging of kidney tumor–bearing mice treated with gemcitabine by DCE-MRI revealed that gemcitabine caused vascular changes both in the tumors and in normal kidneys. Kidney tumors treated with gemcitabine showed improved clearance of the Gd contrast agent relative to the normal contralateral kidney. Increased tumor perfusion caused by gemcitabine was also observed by parametric maps showing uptake of Gd in the core of the tumor in contrast [5]. Histologically, gemcitabine-treated tumors showed a decrease in the number of enlarged vessels compared with control tumors. These findings on improved tumor perfusion associated with trimming of the enlarged vessels of the kidney tumors suggest that gemcitabine also exerted cytotoxic activity on endothelial cells. In agreement with our findings, recent studies demonstrated that endothelial cells are indeed destroyed by gemcitabine both *in vitro* and *in vivo* in an orthotopic preclinical model of pancreatic cancer [44]. These studies and our findings indicate that the mode of action of gemcitabine includes not only cytotoxicity to tumor cells but also an antiangiogenic effect, thus acting as well on the tumor microenvironment as shown for sunitinib [44].

Consistent with our previous studies, sunitinib treatment of kidney tumors with 20 mg/kg showed patterns of uptake and improved Gd clearance by DCE-MRI, comparable to those of normal kidneys, suggesting a return to more normal vasculature with lower permeability (i.e., less leaky vessels) [5]. Histologically, kidney tumors treated with sunitinib showed considerable thinning, regularization, and organization of tumor vessels, as previously reported [5]. With the combination of sunitinib and gemcitabine, the patterns of Gd uptake and clearance resembled those of gemcitabine alone in both kidney tumors and normal kidneys, with a tendency to decreased clearance of Gd. Parametric maps showed increased tumor perfusion. These data were in agreement with *in situ* histologic findings, showing tumor vessels looking more trimmed and organized than those seen after gemcitabine treatment alone.

Quantitation of vascular changes induced by sunitinib and gemcitabine confirmed the reproducibility of our findings. Lower R_{50} values were consistently observed in mice treated with SU20, gemcitabine, and both combined compared with control mice for kidney tumors. A trend to lower R_{50} values was also observed for normal kidneys in treated mice relative to control mice. These findings were corroborated by *in situ* histologic observation of dilatation of some of the vessels in normal kidney tissue sections. These data indicate a relatively mild systemic effect on normal kidney vasculature mediated by either drug alone and both drugs combined. This is in contrast to a more pronounced effect of the therapy on kidney tumor vasculature resulting in increased tumor perfusion and decreased vascular permeability.

Our data suggest that both sunitinib and gemcitabine exert antiangiogenic effects in addition to their cytotoxic antitumor activity. These effects on both the tumor vasculature and tumor cells were observed in both primary kidney tumors and spontaneous lung metastases, indicating that a combined approach of antiangiogenic drug and gemcitabine could be effective for metastatic RCC disease. These studies also emphasize the clinical potential of using DCE-MRI to

select the dose and schedule of antiangiogenic drugs to schedule chemotherapy and improve its efficacy.

Acknowledgments

The authors thank Yimin Shen for excellent technical assistance with DCE-MRI and Andre Konski, Michael Joiner, and Ulka Vaishampayan (Karmanos Cancer Institute) for stimulating discussions on clinical translation issues.

References

[1] Jemal A, Siegel R, Ward E, Hao Y, Xu J, Murray T, and Thun MJ (2008). Cancer statistics, 2008. *CA Cancer J Clin* **58**, 71–96.

[2] Haas GP and Hillman GG (1996). Update on the role of immunotherapy in the management of kidney cancer. *Cancer Control* **3**, 536–541.

[3] Motzer RJ, Bander NH, and Nanus DM (1996). Renal-cell carcinoma. *N Engl J Med* **335**, 865–875.

[4] Motzer RJ, Michaelson MD, Redman BG, Hudes GR, Wilding G, Figlin RA, Ginsberg MS, Kim ST, Baum CM, DePrimo SE, et al. (2006). Activity of SU11248, a multitargeted inhibitor of vascular endothelial growth factor receptor and platelet-derived growth factor receptor, in patients with metastatic renal cell carcinoma. *J Clin Oncol* **24**, 16–24.

[5] Hillman GG, Singh-Gupta V, Zhang H, Al-Bashir AK, Katkuri Y, Li M, Yunker CK, Patel AD, Abrams J, and Haacke EM (2009). Dynamic contrast-enhanced magnetic resonance imaging of vascular changes induced by sunitinib in papillary renal cell carcinoma xenograft tumors. *Neoplasia* **11**, 910–920.

[6] Mendel DB, Laird AD, Xin X, Louie SG, Christensen JG, Li G, Schreck RE, Abrams TJ, Ngai TJ, Lee LB, et al. (2003). *In vivo* antitumor activity of SU11248, a novel tyrosine kinase inhibitor targeting vascular endothelial growth factor and platelet-derived growth factor receptors: determination of a pharmacokinetic/pharmacodynamic relationship. *Clin Cancer Res* **9**, 327–337.

[7] Abrams TJ, Lee LB, Murray LJ, Pryer NK, and Cherrington JM (2003). SU11248 inhibits KIT and platelet-derived growth factor receptor beta in preclinical models of human small cell lung cancer. *Mol Cancer Ther* **2**, 471–478.

[8] Abrams TJ, Murray LJ, Pesenti E, Holway VW, Colombo T, Lee LB, Cherrington JM, and Pryer NK (2003). Preclinical evaluation of the tyrosine kinase inhibitor SU11248 as a single agent and in combination with "standard of care" therapeutic agents for the treatment of breast cancer. *Mol Cancer Ther* **2**, 1011–1021.

[9] Murray LJ, Abrams TJ, Long KR, Ngai TJ, Olson LM, Hong W, Keast PK, Brassard JA, O'Farrell AM, Cherrington JM, et al. (2003). SU11248 inhibits tumor growth and CSF-1R–dependent osteolysis in an experimental breast cancer bone metastasis model. *Clin Exp Metastasis* **20**, 757–766.

[10] O'Farrell AM, Abrams TJ, Yuen HA, Ngai TJ, Louie SG, Yee KW, Wong LM, Hong W, Lee LB, Town A, et al. (2003). SU11248 is a novel FLT3 tyrosine kinase inhibitor with potent activity *in vitro* and *in vivo*. *Blood* **101**, 3597–3605.

[11] Sohal J, Phan VT, Chan PV, Davis EM, Patel B, Kelly LM, Abrams TJ, O'Farrell AM, Gilliland DG, Le Beau MM, et al. (2003). A model of APL with FLT3 mutation is responsive to retinoic acid and a receptor tyrosine kinase inhibitor, SU11657. *Blood* **101**, 3188–3197.

[12] Xu L, Tong R, Cochran DM, and Jain RK (2005). Blocking platelet-derived growth factor-D/platelet-derived growth factor receptor beta signaling inhibits human renal cell carcinoma progression in an orthotopic mouse model. *Cancer Res* **65**, 5711–5719.

[13] Huang D, Ding Y, Li Y, Luo WM, Zhang ZF, Snider J, Vandenbeldt K, Qian CN, and Teh BT (2010). Sunitinib acts primarily on tumor endothelium rather than tumor cells to inhibit the growth of renal cell carcinoma. *Cancer Res* **70**, 1053–1062.

[14] Motzer RJ, Hutson TE, Tomczak P, Michaelson MD, Bukowski RM, Rixe O, Oudard S, Negrier S, Szczylik C, Kim ST, et al. (2007). Sunitinib *versus* interferon α in metastatic renal-cell carcinoma. *N Engl J Med* **356**, 115–124.

[15] Motzer RJ, Hutson TE, Tomczak P, Michaelson MD, Bukowski RM, Oudard S, Negrier S, Szczylik C, Pili R, Bjarnason GA, et al. (2009). Overall survival and updated results for sunitinib compared with interferon α in patients with metastatic renal cell carcinoma. *J Clin Oncol* **27**, 3584–3590.

[16] Kollmannsberger C, Soulieres D, Wong R, Scalera A, Gaspo R, and Bjarnason G (2007). Sunitinib therapy for metastatic renal cell carcinoma: recommendations for management of side effects. *Can Urol Assoc J* **1**, S41–S54.

[17] Chu TF, Rupnick MA, Kerkela R, Dallabrida SM, Zurakowski D, Nguyen L, Woulfe K, Pravda E, Cassiola F, Desai J, et al. (2007). Cardiotoxicity associated with tyrosine kinase inhibitor sunitinib. *Lancet* **370**, 2011–2019.

[18] Telli ML, Witteles RM, Fisher GA, and Srinivas S (2008). Cardiotoxicity associated with the cancer therapeutic agent sunitinib malate. *Ann Oncol* **19**, 1613–1618.

[19] Schmidinger M, Zielinski CC, Vogl UM, Bojic A, Bojic M, Schukro C, Ruhsam M, Hejna M, and Schmidinger H (2008). Cardiac toxicity of sunitinib and sorafenib in patients with metastatic renal cell carcinoma. *J Clin Oncol* **26**, 5204–5212.

[20] Jain RK (2005). Normalization of tumor vasculature: an emerging concept in antiangiogenic therapy. *Science* **307**, 58–62.

[21] Jain RK (2001). Normalizing tumor vasculature with anti-angiogenic therapy: a new paradigm for combination therapy. *Nat Med* **7**, 987–989.

[22] Yankeelov TE, Lepage M, Chakravarthy A, Broome EE, Niermann KJ, Kelley MC, Meszoely I, Mayer IA, Herman CR, McManus K, et al. (2007). Integration of quantitative DCE-MRI and ADC mapping to monitor treatment response in human breast cancer: initial results. *Magn Reson Imaging* **25**, 1–13.

[23] Jackson A, O'Connor JP, Parker GJ, and Jayson GC (2007). Imaging tumor vascular heterogeneity and angiogenesis using dynamic contrast-enhanced magnetic resonance imaging. *Clin Cancer Res* **13**, 3449–3459.

[24] Hahn OM, Yang C, Medved M, Karczmar G, Kistner E, Karrison T, Manchen E, Mitchell M, Ratain MJ, and Stadler WM (2008). Dynamic contrast-enhanced magnetic resonance imaging pharmacodynamic biomarker study of sorafenib in metastatic renal carcinoma. *J Clin Oncol* **26**, 4572–4578.

[25] Hylton N (2006). Dynamic contrast-enhanced magnetic resonance imaging as an imaging biomarker. *J Clin Oncol* **24**, 3293–3298.

[26] Checkley D, Tessier JJ, Kendrew J, Waterton JC, and Wedge SR (2003). Use of dynamic contrast-enhanced MRI to evaluate acute treatment with ZD6474, a VEGF signalling inhibitor, in PC-3 prostate tumours. *Br J Cancer* **89**, 1889–1895.

[27] Marzola P, Degrassi A, Calderan L, Farace P, Nicolato E, Crescimanno C, Sandri M, Giusti A, Pesenti E, Terron A, et al. (2005). Early antiangiogenic activity of SU11248 evaluated *in vivo* by dynamic contrast-enhanced magnetic resonance imaging in an experimental model of colon carcinoma. *Clin Cancer Res* **11**, 5827–5832.

[28] Desai AA, Vogelzang NJ, Rini BI, Ansari R, Krauss S, and Stadler WM (2002). A high rate of venous thromboembolism in a multi-institutional phase II trial of weekly intravenous gemcitabine with continuous infusion fluorouracil and daily thalidomide in patients with metastatic renal cell carcinoma. *Cancer* **95**, 1629–1636.

[29] Tannir NM, Thall PF, Ng CS, Wang X, Wooten L, Siefker-Radtke A, Mathew P, Pagliaro L, Wood C, and Jonasch E (2008). A phase II trial of gemcitabine plus capecitabine for metastatic renal cell cancer previously treated with immunotherapy and targeted agents. *J Urol* **180**, 867–872.

[30] Amato RJ and Khan M (2008). A phase I clinical trial of low-dose interferon-α-2A, thalidomide plus gemcitabine and capecitabine for patients with progressive metastatic renal cell carcinoma. *Cancer Chemother Pharmacol* **61**, 1069–1073.

[31] Perez-Zincer F, Olencki T, Budd GT, Peereboom D, Elson P, and Bukowski RM (2002). A phase I trial of weekly gemcitabine and subcutaneous interferon α in patients with refractory renal cell carcinoma. *Invest New Drugs* **20**, 305–310.

[32] Hillman GG, Wang Y, Che M, Raffoul JJ, Yudelev M, Kucuk O, and Sarkar FH (2007). Progression of renal cell carcinoma is inhibited by genistein and radiation in an orthotopic model. *BMC Cancer* **7**, 4.

[33] Hillman GG, Wang Y, Kucuk O, Che M, Doerge DR, Yudelev M, Joiner MC, Marples B, Forman JD, and Sarkar FH (2004). Genistein potentiates inhibition of tumor growth by radiation in a prostate cancer orthotopic model. *Mol Cancer Ther* **3**, 1271–1279.

[34] Haacke EM, Filleti CL, Gattu R, Ciulla C, Al-Bashir A, Suryanarayanan K, Li M, Latif Z, DelProposto Z, Sehgal V, et al. (2007). New algorithm for quantifying vascular changes in dynamic contrast-enhanced MRI independent of absolute T1 values. *Magn Reson Med* **58**, 463–472.

[35] Raffoul JJ, Banerjee S, Singh-Gupta V, Knoll ZE, Fite A, Zhang H, Abrams J, Sarkar FH, and Hillman GG (2007). Down-regulation of apurinic/apyrimidinic endonuclease 1/redox factor-1 expression by soy isoflavones enhances prostate cancer radiotherapy *in vitro* and *in vivo*. *Cancer Res* **67**, 2141–2149.

[36] Holm S (2009). A simple sequentially rejective multiple test procedure. *Scand J Statist* **6**, 65–70.

[37] Browder T, Butterfield CE, Kraling BM, Shi B, Marshall B, O'Reilly MS, and Folkman J (2000). Antiangiogenic scheduling of chemotherapy improves efficacy against experimental drug-resistant cancer. *Cancer Res* **60**, 1878–1886.

[38] Klement G, Baruchel S, Rak J, Man S, Clark K, Hicklin DJ, Bohlen P, and Kerbel RS (2000). Continuous low-dose therapy with vinblastine and VEGF receptor-2 antibody induces sustained tumor regression without overt toxicity. *J Clin Invest* **105**, R15–R24.

[39] Wildiers H, Guetens G, De Boeck G, Verbeken E, Landuyt B, Landuyt W, de Bruijn EA, and van Oosterom AT (2003). Effect of antivascular endothelial growth factor treatment on the intratumoral uptake of CPT-11. *Br J Cancer* **88**, 1979–1986.

[40] Bocci G, Danesi R, Marangoni G, Fioravanti A, Boggi U, Esposito I, Fasciani A, Boschi E, Campani D, Bevilacqua G, et al. (2004). Antiangiogenic *versus* cytotoxic therapeutic approaches to human pancreas cancer: an experimental study with a vascular endothelial growth factor receptor-2 tyrosine kinase inhibitor and gemcitabine. *Eur J Pharmacol* **498**, 9–18.

[41] Ah-See ML, Makris A, Taylor NJ, Harrison M, Richman PI, Burcombe RJ, Stirling JJ, d'Arcy JA, Collins DJ, Pittam MR, et al. (2008). Early changes in functional dynamic magnetic resonance imaging predict for pathologic response to neoadjuvant chemotherapy in primary breast cancer. *Clin Cancer Res* **14**, 6580–6589.

[42] Galban CJ, Chenevert TL, Meyer CR, Tsien C, Lawrence TS, Hamstra DA, Junck L, Sundgren PC, Johnson TD, Ross DJ, et al. (2009). The parametric response map is an imaging biomarker for early cancer treatment outcome. *Nat Med* **15**, 572–576.

[43] Craciunescu OI, Blackwell KL, Jones EL, Macfall JR, Yu D, Vujaskovic Z, Wong TZ, Liotcheva V, Rosen EL, Prosnitz LR, et al. (2009). DCE-MRI parameters have potential to predict response of locally advanced breast cancer patients to neoadjuvant chemotherapy and hyperthermia: a pilot study. *Int J Hyperthermia* **25**, 405–415.

[44] Laquente B, Lacasa C, Ginesta MM, Casanovas O, Figueras A, Galan M, Ribas IG, Germa JR, Capella G, and Vinals F (2008). Antiangiogenic effect of gemcitabine following metronomic administration in a pancreas cancer model. *Mol Cancer Ther* **7**, 638–647.